



Assessment of neutron irradiation effects on RAFM steels

Ermile Gaganidze*, Jarir Aktaa

Karlsruher Institut für Technologie, Institut für Angewandte Materialien, Hermann-von-Helmholtz-Platz 1, D-76344 Eggenstein-Leopoldshafen, Germany

HIGHLIGHTS

- The effects of the neutron irradiation on the mechanical properties of RAFM steels are assessed up to 80 dpa.
- The impacts of helium on the mechanical properties and swelling are estimated by reviewing helium simulating experiments.
- The recommendations for the operating conditions are given for fusion reactor First Wall and blanket structural materials.

ARTICLE INFO

Article history:

Received 2 August 2012

Received in revised form 5 November 2012

Accepted 24 November 2012

Available online 27 December 2012

Keywords:

Structural materials

RAFM steels

Irradiation damage

Helium effects

ABSTRACT

The objective of the current work is assessment of the effects of neutron irradiation on the mechanical properties of blanket and divertor materials of a future fusion energy generation Demonstration Power Plant (DEMO). The emphasis is put on the review of the tensile, Charpy impact and fracture toughness properties of EUROFER97 and EUROFER ODS (9%Cr) steels irradiated up to a displacement damage dose of 80 dpa in order to address (i) irradiation dose dependence of mechanical properties, (ii) irradiation temperature dependence of the mechanical properties, (iii) helium effects on the mechanical properties. The assessment will be used to give recommendations on the operating temperature range for the First Wall and helium cooled Breeding Blanket materials and to identify needs for structural materials R&D.

© 2013 Karlsruhe Institute of Technology (KIT). Published by Elsevier B.V. All rights reserved.

1. Introduction

Structural materials for in-vessel components of future energy generating fusion reactors (FR) will be exposed to high neutron and thermo-mechanical loads. Degradation of microstructure of structural materials under neutron irradiation as a result of displacement damage accumulation up to damage doses of 150 dpa and production of transmutation products, i.e. helium and hydrogen will strongly influence materials' performance. The reduced activation ferritic/martensitic (RAFM) steels and their oxide dispersion strengthened (ODS) variants are considered as primary candidate structural materials for the First Wall (FW) and helium cooled Breeding Blanket (BB) with operating temperature range between 350 and 650 °C [1]. In addition the supporting structure for the cooling finger units of a helium cooled divertor will be made out of ODS RAFM steel [2]. The irradiation hardening at low temperatures (<350 °C), accompanied by embrittlement and reduced ductility remain the limiting factors for material application, indicating further needs of material development as well as new approaches in BB design optimization [3].

The European RAFM steel EUROFER97 emerged in the course of the European application driven material development programme [4] and represents the European reference structural steel for the FW and BB of a future fusion energy generation Demonstration Power Plant (DEMO). A large characterization programme has been performed including microstructural, mechanical and corrosion experiments. Since a simulation facility with fusion reactor relevant neutron spectrum, like IFMIF, is not yet available, the irradiation behaviour of EUROFER97 and its ODS variants was investigated in several irradiation programmes performed in various Material Test Reactors [5–12]. The current work aimed at assessment of the mechanical properties of neutron irradiated RAFM steels. The emphasis was put on the assessment of tensile, Charpy impact and fracture toughness properties of EUROFER97 and EUROFER ODS (9%Cr) steels irradiated up to a displacement damage dose of 80 dpa. The effects of the neutron irradiation temperature and dose were investigated. For comparative purpose irradiation performance of the selected international RAFM steels has been also considered. The impact of helium on the mechanical properties and swelling has been assessed by reviewing the results obtained by selected helium simulating techniques. The recommendations for the operating temperature and dpa range for the First Wall and blanket materials are given and needs for structural materials R&D are identified.

* Corresponding author. Tel.: +49 721 608 24083; fax: +49 721 608 24566.
E-mail address: ermile.gaganidze@kit.edu (E. Gaganidze).

2. Materials

An attention was paid to a clear identification of materials regarding manufacturer, batch number, chemical composition and thermal or thermo-mechanical heat treatment history.

2.1. EUROFER97

An industrial batch of the European RAFM steel EUROFER97 (nominal composition Fe–9Cr–1.1W–0.2V–0.12Ta) was produced by Böhler Austria GmbH. Four different product forms, i.e. plates with thicknesses of 8, 14 (Heat E83698) and 25 mm (Heat E83697) and bars of 100 mm in diameter (Heat E83699), were distributed by the Karlsruhe Institute of Technology (KIT) (formerly Forschungszentrum Karlsruhe – FZK) to different European associations. Producer austenization was performed at 980 °C/0.5 h and tempering, followed by air cooling was done at 760 °C/1.5 h for the plates and at 740 °C/3.7 h for the bars. Chemical composition of EUROFER97 and other selected RAFM steels are summarized in Table 1. For the case of 25 mm EUROFER97 plate (Heat E83697) the influence of a laboratory scale heat treatment (HT) was studied by KIT. Namely, part of the specimens (referred to as EUROFER97) was machined from 25 mm EUROFER97 plates in the as-delivered state. Another part of the specimens (referred to as EUROFER97 HT) was machined from 25 mm EUROFER97 plates which in addition to a HT by the producer at (980 °C/0.5 h + 760 °C/1.5 h) were subjected to a laboratory-scale pre-irradiation HT of (1040 °C/38 min + 750 °C/2 h).

2.2. Reference RAFM steels

5 tonnes heat of modified F82H (F82H-mod, nominal composition Fe–7.5Cr–2W–0.15V–0.02Ta–0.1C) was produced by NKK Corporation (Japan) for collaborative research coordinated by the International Energy Agency (IEA) implementing agreement on Fusion Materials (Annex-II). 7.5, 15 (Heat 9741) and 25 mm (Heat 9753) plates were distributed by IEA and subsequently by KIT to the European partners. Producer austenization at 1040 °C/38 min on 7.5 and 15 mm plates and at 1040 °C/40 min on 25 mm plates was followed by tempering at 750 °C/1 h. KIT performed a laboratory-scale pre-irradiation HT of 950 °C/30 min + 750 °C/2 h on 8 mm plate (Heat 9741) and a laboratory-scale pre-irradiation HT of 1040 °C/38 min + 750 °C/2 h on the 25 mm plate (Heat 9753). The Nuclear Research and Consultancy Group (NRG) Petten, investigated the 25 mm plate both in as-received and optimum heat-treated condition for impact toughness 920 °C/30 min + 730 °C/2 h. The 7.5 and 15 mm F82H-mod plates were studied by NRG in as-received state.

The German development OPTIFER Ia (Heat 664, 900 °C/30 min/air cooled + 780 °C/120 min/air cooled), OPTIFER IVc (Heat 986779, labelled OPT IVc) (950 °C/30 min/air cooled + 750 °C/120 min/air cooled) as well as recent developments of OPTIFER series alloys, i.e. OPTIFER XI (labelled OPT XI) (Heat 847, 950 °C/30 min/air cooled + 750 °C/120 min/air cooled) and OPTIFER XII (labelled OPT XII) (Heat 848, 950 °C/30 min/air cooled + 750 °C/120 min/air cooled) were also intensively studied in several European irradiation programmes. NRG contributed with NRG 9CrWVTa Eurofer lab heat (labelled BS-EUROF, Heat VS3102) and with NRG 9Cr2WVTa lab heat (Heat VS3104). The both heats were manufactured by British Steel. The final HT performed by manufacturer involved austenization at 1050 °C/60 min followed by air cooling and tempering at 750 °C/120 min followed by air cooling. JLF1 (Fe–9Cr–2W–0.18V–0.08Ta) material from Nippon steel (Heat 449) with manufacturer HT of 1050 °C/60 min + 780 °C/60 min was also studied in European irradiation programmes.

Table 1
Material chemical composition in wt.%(Fe balance).

| Material | Heat | Cr | C | Si | Mn | P | S | Mo | Ni | B | Cu | N | O | Nb | Ti | V | W | Ta |
|--|-------------|-------|-------|-------|-------|--------|--------|---------|--------|--------|--------|--------|--------|---------|---------|-------|-------|-------|
| EUROFER97 | E83697 | 8.93 | 0.12 | 0.06 | 0.47 | <0.005 | 0.004 | 0.0015 | 0.022 | <0.001 | 0.0036 | 0.018 | 0.0008 | 0.0022 | 0.009 | 0.20 | 1.07 | 0.14 |
| EUROFER97 | E83699 | 8.92 | 0.10 | 0.05 | 0.38 | <0.005 | 0.003 | 0.0012 | 0.020 | <0.001 | 0.0037 | 0.027 | 0.013 | <0.001 | 0.006 | 0.19 | 1.09 | 0.078 |
| EUROFER97 | E83698 | 8.82 | 0.11 | 0.04 | 0.47 | 0.005 | 0.004 | <0.0010 | 0.020 | <0.001 | 0.0016 | 0.020 | 0.0010 | 0.0016 | 0.005 | 0.20 | 1.09 | 0.13 |
| F82H-mod | 9753 | 7.89 | 0.09 | 0.08 | 0.1 | 0.003 | 0.001 | 0.003 | 0.02 | 0.0002 | 0.01 | 0.006 | - | 0.0002 | 0.004 | 0.19 | 1.99 | 0.02 |
| OPTIFER Ia | 664 | 9.33 | 0.10 | 0.06 | 0.50 | 0.0046 | 0.005 | 0.005 | 0.005 | 0.0004 | 0.0063 | 0.0153 | 0.0047 | 0.0101 | 0.007 | 0.26 | 0.965 | 0.066 |
| OPTIFER IVc | 986779 | 9.35 | 0.12 | 0.022 | 0.54 | 0.004 | 0.003 | <0.002 | 0.0073 | <0.004 | 0.0019 | 0.05 | 0.0190 | <0.0006 | <0.0004 | 0.26 | 1.03 | 0.07 |
| OPTIFER XI | 847 | 10.1 | 0.1 | 0.035 | 0.532 | 0.001 | 0.0015 | 0.005 | 0.005 | 0.0008 | - | 0.0405 | 0.0143 | 0.001 | 0.001 | 0.20 | 1.11 | 0.055 |
| OPTIFER XII | 848 | 10.65 | 0.11 | 0.153 | 0.464 | 0.0012 | 0.0015 | - | - | 0.0008 | - | 0.051 | 0.0107 | - | - | 0.195 | 1.13 | 0.070 |
| ADS2 | 806 | 9.31 | 0.109 | 0.02 | 0.602 | 0.0035 | 0.003 | 0.002 | 0.005 | 0.0082 | 0.005 | 0.021 | 0.013 | 0.005 | 0.001 | 0.19 | 1.27 | 0.055 |
| ADS3 | 826 | 8.8 | 0.095 | 0.031 | 0.395 | 0.0024 | 0.003 | 0.046 | 0.008 | 0.0083 | 0.006 | 0.028 | 0.0045 | 0.005 | 0.001 | 0.193 | 1.125 | 0.088 |
| ADS4 | 825 | 9.0 | 0.1 | 0.03 | 0.38 | 0.001 | 0.0025 | 0.028 | 0.006 | 0.112 | 0.005 | 0.0255 | 0.0037 | 0.002 | 0.001 | 0.197 | 1.06 | 0.08 |
| EURODSHIP = EUROFER97 + 0.5% Y ₂ O ₃ | HXN 958/3 | 9.4 | 0.11 | 0.12 | 0.42 | 0.04 | 0.004 | 0.007 | 0.07 | <0.005 | 0.015 | 0.029 | 0.171 | 0.001 | 0.001 | 0.19 | 1.10 | 0.08 |
| EODSHIP 3 = EUROFER97 + 0.3 wt.% Y ₂ O ₃ | HXN 954/4-3 | 8.94 | 0.11 | 0.08 | 0.37 | 0.007 | 0.004 | 0.007 | 0.03 | <0.001 | 0.018 | 0.027 | 0.0029 | 0.001 | 0.006 | 0.19 | 1.07 | 0.87 |
| EUROFER-EB | E83697 | 8.93 | 0.12 | 0.06 | 0.47 | <0.005 | 0.004 | 0.0015 | 0.022 | <0.001 | 0.0036 | 0.018 | 0.0008 | 0.0022 | 0.009 | 0.20 | 1.07 | 0.14 |

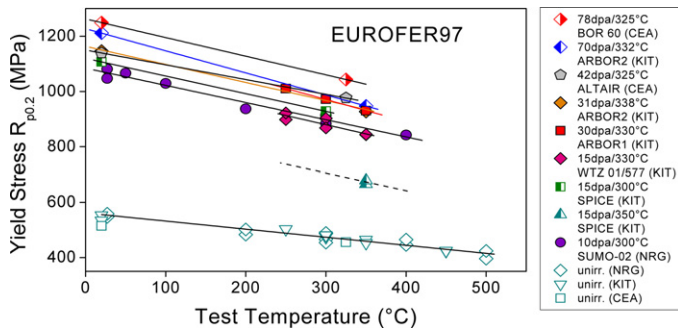


Fig. 1. Yield Stress vs. test temperature for EUROFER97 in the unirradiated condition and after neutron irradiations in different European irradiation programmes. The lines are guide for the eye.

programmes KIT investigated medium and high dose impact, tensile and LCF properties of EUROFER97 (Heat 83697), EUROFER97 HT (Heat 83697), EUROFER ODS steels (Heats HXN 958/3, HXN 954/4-3) and other reference RAFM steels. Irradiation programme SPICE was performed in the High Flux Reactor (HFR) in Petten [7,8]. The emphasis was put on the investigation of influence of the irradiation temperature on the mechanical properties of RAFM steels. The specimens were irradiated to a target dose of 15 dpa at multiple target temperatures of 250, 300, 350, 400, and 450 $^{\circ}\text{C}$. Irradiation programmes WIZ-01/577, ARBOR 1 and ARBOR 2 were performed in the BOR 60 fast reactor at Joint Stock Company (JSC) "State Scientific Centre Research Institute of Atomic Reactors" (SSC RIAR) to target damage doses of 15, 32 and 70 dpa, respectively. The irradiation temperatures were between 330 and 338 $^{\circ}\text{C}$. In addition to EUROFER97 in SPICE and ARBOR irradiation programmes KIT irradiated seven reference RAFM steels as well as three boron doped RAFM steels. Within SPICE programme KIT studied irradiation behaviour of F82H-mod 8 mm plates (Heat 9741), whereas within ARBOR 1 and ARBOR 2 programmes the irradiation behaviour of F82H-mod 25 mm plate (Heat 9753) was investigated.

Irradiation performance of EUROFER97 (Heat E83698) and other selected RAFM steels, e.g. NRG 9Cr2WVTa lab heat (VS3104), JLF1 (Heat 449) and EUROFER ODS (Heat LXN0449), was investigated by the French Alternative Energies and Atomic Energy Commission (CEA) within irradiation experiments performed in the BOR 60 fast reactor of SSC RIAR. Within ALTAIR programme the specimens were irradiated to damage doses between 32 and 40 dpa at 325 \pm 5 $^{\circ}\text{C}$ [10]. Some of the specimens irradiated in ALTAIR were re-irradiated at 325 $^{\circ}\text{C}$ up to a cumulative damage dose of 78 dpa in BOR 60 as part of the joint KIT-CEA ARBOR 2 experiment [12].

4. Tensile properties

Fig. 1 shows Yield Stress ($R_{p0.2}$) vs. test temperature (T_{test}) for EUROFER97 in the unirradiated condition and after neutron irradiation in different medium and high dose European irradiation programmes at target irradiation temperatures (T_{irr}) between 300 and 350 $^{\circ}\text{C}$ [6,8–12]. In addition to tensile data compilation performed in [18,11] the current diagram also includes recent results from [12]. Tensile tests were performed on five different specimen types as can be inferred from Table 2. The tensile tests performed by NRG, KIT and CEA on unirradiated EUROFER97 are in a narrow scatter band concerning the Yield Stresses and give a good basis for the interpretation of the tensile results.

Neutron irradiation leads to substantial increases in the Yield Stress which is sensitive to the irradiation parameters, i.e. irradiation dose and temperature. Furthermore, for given irradiation conditions the Yield Stress increase depends on the test

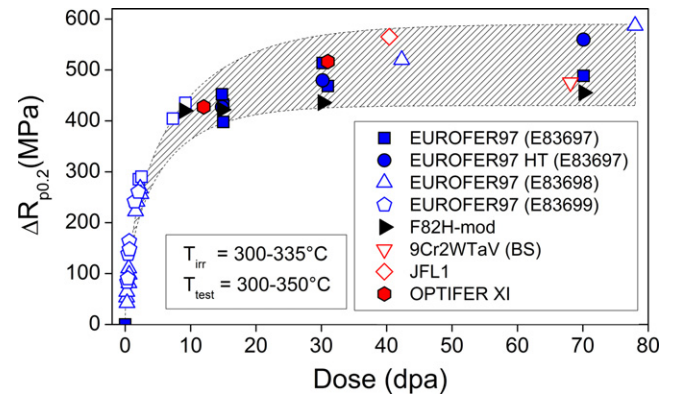


Fig. 2. Irradiation hardening vs. irradiation dose for EUROFER97 and other RAFM steels for $T_{\text{irr}} = 300\text{--}335^{\circ}\text{C}$ and $T_{\text{test}} = 300\text{--}350^{\circ}\text{C}$. The full symbols represent KIT results [8,9,11,17]. The open symbols are from different European irradiation experiments carried out by SCK-CEN, NRG, CEA [5,6,10,12,18]. The hatched area marks the scattering band for high dose results and is guide for the eye.

temperature and is larger at low test temperatures. The specimens irradiated to 78 dpa in BOR 60 show the highest Yield Stresses at test temperatures of 20 and 325 $^{\circ}\text{C}$. While the differences in the Yield Stress values at 300 and 330 $^{\circ}\text{C}$ irradiations to 15 dpa are still moderate and within data scatter, as can be seen from the comparison between WIZ 01/577 [17] and SPICE [8] results, Yield Stress values after irradiation to 15 dpa at 350 $^{\circ}\text{C}$ (SPICE [8]) are considerably lower indicating substantial recovery of radiation defects at this irradiation temperature. The test temperature and dose dependences of the Ultimate Tensile Strength (R_m) resembles to that of the Yield Stress [11]. Close values of the Ultimate Tensile Strength (R_m) and Yield Stress ($R_{p0.2}$) in the irradiated conditions indicate a strong suppression of the strain hardening capability under neutron irradiation.

The evolution of the hardening, as the increase in Yield Stress, with damage dose for different product forms of EUROFER97 and for other selected RAFM steels for $T_{\text{irr}} = 300\text{--}335^{\circ}\text{C}$ and $T_{\text{test}} = 300\text{--}350^{\circ}\text{C}$ is summarized in Fig. 2. KIT results from SPICE [8], WIZ 01/577 [17], ARBOR 1 [9] and ARBOR 2 [11] irradiation programmes are represented by solid symbols. The open symbols represent available results from the literature [5,6,10,12,18]. A detailed assessment of low and medium dose (up to 10 dpa) tensile properties of EUROFER97 was performed in [19,20]. Neutron irradiation leads to a substantial increase in the Yield Stress of RAFM steels with the damage dose. The Yield Stress increase is rather steep at doses below 10 dpa. The hardening rate appears to be significantly decreased at the achieved damage doses and a clear tendency towards saturation is identified. It was shown in [3] that the dose evolution of hardening of RAFM steels can be qualitatively described within Whapham and Makin model [21]. For the analysis of high dose irradiation behaviour of EUROFER97 differentiation has to be done between different product forms as well as different heat treatment conditions. The plate material investigated in CEA experiments (Heat E83698, 8 mm plate) differ from that studied in other medium and high dose experiments (damage dose ≥ 2.5 dpa in Fig. 2) where specimens were manufactured from 25 mm plates (Heat E83697). A considerably larger Yield Stress increase observed at 78 dpa (Heat E83698, 8 mm plate) in comparison to a Yield Stress increase measured at 70 dpa (Heat E83697, 25 mm plate) indicates a strong sensitivity of materials' mechanical properties and irradiation performance to metallurgical parameters. The effect of different specimen orientations used in KIT and CEA experiments is not clear, either. Furthermore, the results on EUROFER97 HT (Heat E83697) reveals that the austenization at a temperature of 1040 $^{\circ}\text{C}$ performed at laboratory scale by KIT has

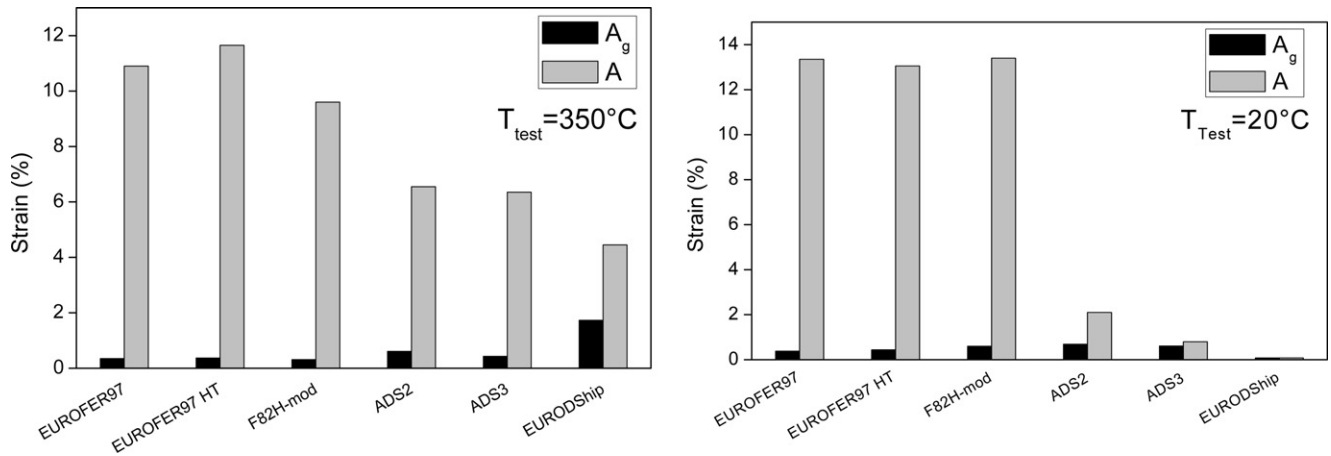


Fig. 3. Uniform Strain (A_g) and Fracture Strain (A) of 70.1 dpa, 331.5 °C irradiated RAFM materials tested at 350 °C (left) and 20 °C (right) [11].

a remarkable influence on the hardening behaviour, i.e. at a damage dose of 70 dpa hardening shown by EUROFER97 HT is approx. 70 MPa larger than hardening shown by EUROFER97 (Heat E83697).

Hardening quantified for F82H-mod and 9Cr2W1TaV (British Steel, Heat VS3104) at 70 dpa is comparable to that of EUROFER97 (Heat E83697). Furthermore, F82H-mod indicates saturation of hardening at achieved damage doses. The hatched area marks the scattering band of high dose hardening for different RAFM steels. It is important to note that to the reasons for the data scattering belong not only the differences in the metallurgical variables, but also variations and uncertainties in the irradiation conditions. The limited number of available irradiated specimens does not allow detailed statistical analysis of the results.

Fig. 3 shows Uniform Strain and Fracture Strain of selected RAFM steel specimens irradiated to 70.1 dpa at 331.5 °C and tested at 350 and 20 °C [11]. Rather low values of the Uniform Strains below 1% are observed for all investigated RAFM steels. The Fracture Strains, in contrast, remain at a high level above 9–10%. The boron doped steels show larger Uniform and reduced Fracture Strains in comparison to base RAFM steels. We remind that *approximately* 24 and 120 appm B were produced after irradiation of ADS2 and ADS3 steels in BOR 60 up to 70 dpa [22]. Among all investigated steels the ODS EUROFER (HXN 958/3) shows the largest value of the Uniform Strain of 1.73% at a test temperature of 350 °C. The Fracture and Uniform Strain of irradiated ODS EUROFER (HXN 958/3) fell however down to 0.08% at a test temperature of 20 °C. A similar suppression of elongation properties at a test temperature of 20 °C was observed for hot extruded EUROFER ODS (Heat LXN0449) after irradiation to 40.4 dpa at 325 °C in [12].

A correlation between ductility parameters of stainless steels was studied in [23]. A rough linear relationship of type

$$A_g = \left(1 - \frac{R_{p0.2}}{R_m}\right) \quad (1)$$

was found between the Uniform Strain (A_g) and strain hardening capability ($R_{p0.2}/R_m$) for unirradiated and irradiated stainless steels [23]. Such empirical relationship was considered to be useful for prediction of the ductility properties from the strength properties.

The evolution of elongation properties with irradiation dose for different product forms of EUROFER97 for irradiation temperatures between 300 and 335 °C and test temperatures between 300 and 350 °C is shown in Fig. 4. The both tensile properties show a strong reduction from their values in the reference unirradiated state already at a damage dose of 2.1 dpa. The Uniform Strain (A_g) is scattered mostly below 0.5% in the irradiated state. Though strongly

reduced, the Fracture Strain (A) remains mostly at or above 10% for irradiated specimens. The exceptions are CEA specimens which exhibit Fracture Strain of about 6% in the irradiated state both at 42 and 78 dpa. The circles in Fig. 4 show semi-empirical description of Uniform Strain with Eq. (1). The empirical equation provides good description of the Uniform Strain in the irradiated state indicating that strong reduction of the Uniform Strain is closely correlated to a strong suppression of strain hardening capability.

5. Impact properties

The role of irradiation temperature on the impact properties of EUROFER97 and other RAFM steels was studied in SPICE programme [7]. Fig. 5 shows the DBTT vs. irradiation temperature for EUROFER97 and other RAFM steels from SPICE irradiation. The damage doses achieved at 250 and 300 °C within SPICE programme were 13.6 and 14.8 dpa respectively and a damage dose averaged over doses achieved at all target temperatures was 16.3 dpa. For comparison the result obtained on EUROFER97 after irradiation to 15 dpa at 330 °C within WTZ programme [17] is also included in Fig. 5. The DBTT of all steels is influenced most at low irradiation temperatures ($T_{irr} \leq 330^\circ\text{C}$). The DBTTs of the materials irradiated at or above 350 °C remain below -24°C and, hence, are well below the material application temperature. On the basis of this diagram a temperature window between 350 and 550 °C is proposed for operation of the FW and Blanket components.

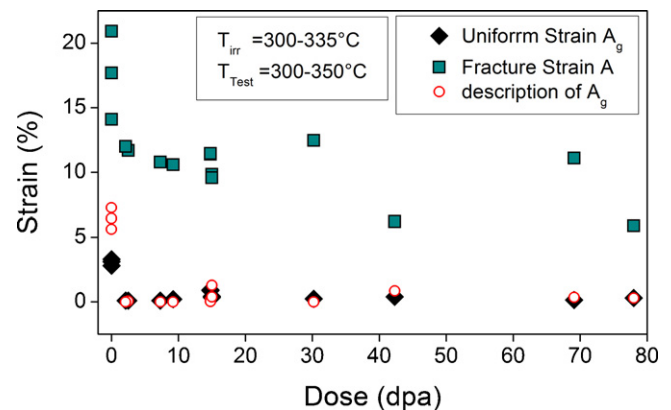


Fig. 4. Uniform and Fracture Strain vs. damage dose for different product forms of EUROFER97 compiled from [6,8–12]. The circles represent the semi-empirical description of Uniform Strain with Eq. (1).

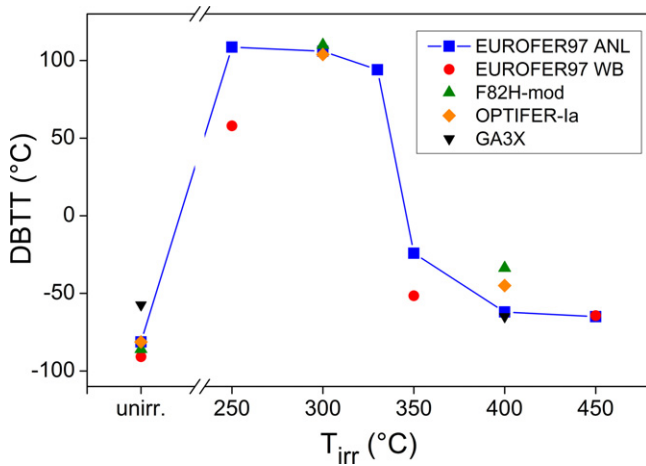


Fig. 5. DBTT vs. irradiation temperature for selected RAFM steels from SPICE [7,43]. Average damage dose in SPICE was 16.3 dpa. For comparison, the results obtained in the unirradiated conditions are also included. The data point at $T_{irr} = 330^\circ\text{C}$ (15 dpa) is from WTZ programme [17].

The influence of the irradiation temperature (300, 450, 550 °C) on the impact properties of recent development ODS EUROFER steel up to a damage dose of 3 dpa was studied in [14]. Significant DBTT shifts of 56 °C and 151 °C were reported after irradiation at 300 °C to 1 and 3 dpa, respectively [14]. The DBTT shifts after irradiation at 450 and 550 °C were in contrast marginal.

Fig. 6 shows the evolution of the neutron irradiation induced embrittlement (measured in impact tests) with dose for EUROFER97 and F82H steels at irradiation temperatures between 300 and 337 °C [24,11]. For comparison the results from [6,10,12] as well as neutron irradiation induced embrittlement for OPTIFER [11] and 9Cr2WVTa (BS) [12] steels are also included. In case of EUROFER97, differentiation is made between specimens machined from as-delivered products and specimens machined from the plates subjected to pre-irradiation heat treatment (HT). The results on F82H and F82H-mod are plotted together for different heat treatments and material compositions. The pre-irradiation HT of EUROFER97 leads to considerable improvement of the irradiation resistance at doses up to 30 dpa. At the achieved damage doses, however, the embrittlement of EUROFER97 HT becomes comparable to that of EUROFER97. All RAFM steels show steep increase in the ΔDBTT with dose below 15 dpa. With further increasing the

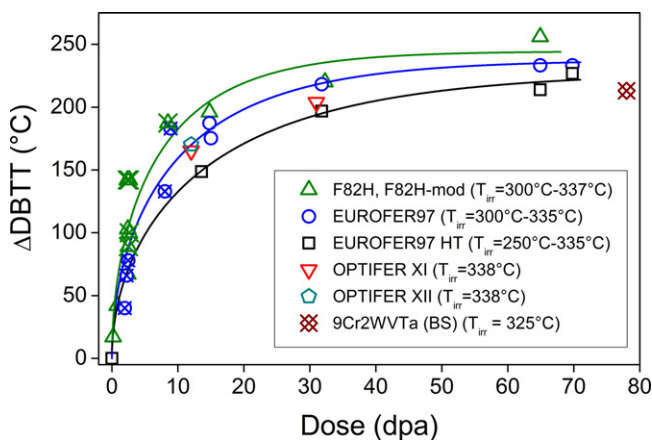


Fig. 6. Irradiation shifts of the DBTT vs. dose for EUROFER97 and other RAFM steels. The open symbols represent KIT results [3,7,9,11,17] and the crossed symbols are from [6,10,12]. The solid lines are a model description of the data [3].

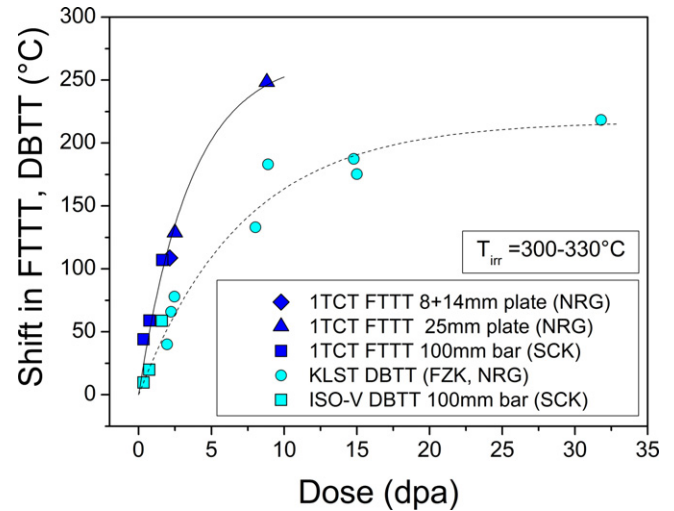


Fig. 7. Irradiation induced shift in Fracture Toughness Transition Temperature (FTTT) and KLST and ISO-V Ductile-to-Brittle Transition Temperature (DBTT) for EUROFER97 vs. irradiation dose [25]. The lines are the least square fits of the results with a function of type $\Delta T_0 = A[1 - \exp(-\text{dose}/\tau)]$, with A and τ being the fitting parameter. The best fits were obtained with $A = 268.9^\circ\text{C}$ and $\tau = 3.58$ dpa for FTTT and with $A = 217.23^\circ\text{C}$ and $\tau = 7.15$ dpa for DBTT.

damage dose the embrittlement rate decreases and a clear tendency towards saturation is observed at the achieved damage doses. F82H-mod irradiated to 65 dpa/337 °C behaves somewhat poorly compared to the EUROFER steels with respect to DBTT increase. The high dose embrittlement of 9Cr2WVTa (BS) steel is comparable but slightly better than that of EUROFER97. The embrittlement of OPTIFER XI and OPTIFER XII after irradiation to 12 dpa (and 31 dpa in case of OPTIFER XI) confirms the embrittlement trend of EUROFER97 steels. The solid lines are a model description of the data [3].

Early development oxide dispersion strengthened EODShip 3 (Heat HXN 954/4-3) and EUODShip (Heat HXN 958/3) steels showed strong degradation of the impact properties at high damage doses [11]. EUROFER ODS steel consolidated by hot extrusion (Heat LXN0449) showed improved unirradiated impact properties [12] in comparison to early development ODS EUROFER steels. The neutron irradiation to 40 dpa, however, lead to a larger DBTT shift and stronger suppression of upper shelf toughness in comparison to base EUROFER steel [12] indicating a need for further material optimization.

6. Fracture Mechanical properties of EUROFER97

Fracture Mechanical (FM) properties of EUROFER97 and other RAFM steels have been intensively studied by NRG [6] and SCK [5] up to damage doses of 10 dpa. Compilation and detailed assessment of FM experiments on irradiated EUROFER97 and F82H specimens was performed in [25]. ASTM E1921-05 procedure was applied to the 1 T normalized data to determine the Fracture Toughness Transition Temperature (FTTT). Fig. 7 shows the neutron irradiation induced shift in FTTT and KLST and ISO-V DBTT for EUROFER97 vs. irradiation dose [25]. Progressive material embrittlement observed for EUROFER97 indicate no saturation of FTTT for the achieved damage doses. Irradiation induced shifts in FTTT are significantly larger than shifts in Charpy DBTT which indicates a non-conservative estimations of the embrittlement by Charpy tests. The lack of high dose data on FTTT of EUROFER97 does not allow prediction of high dose behaviour of FTTT and indicates the need for high dose fracture mechanical experiments.

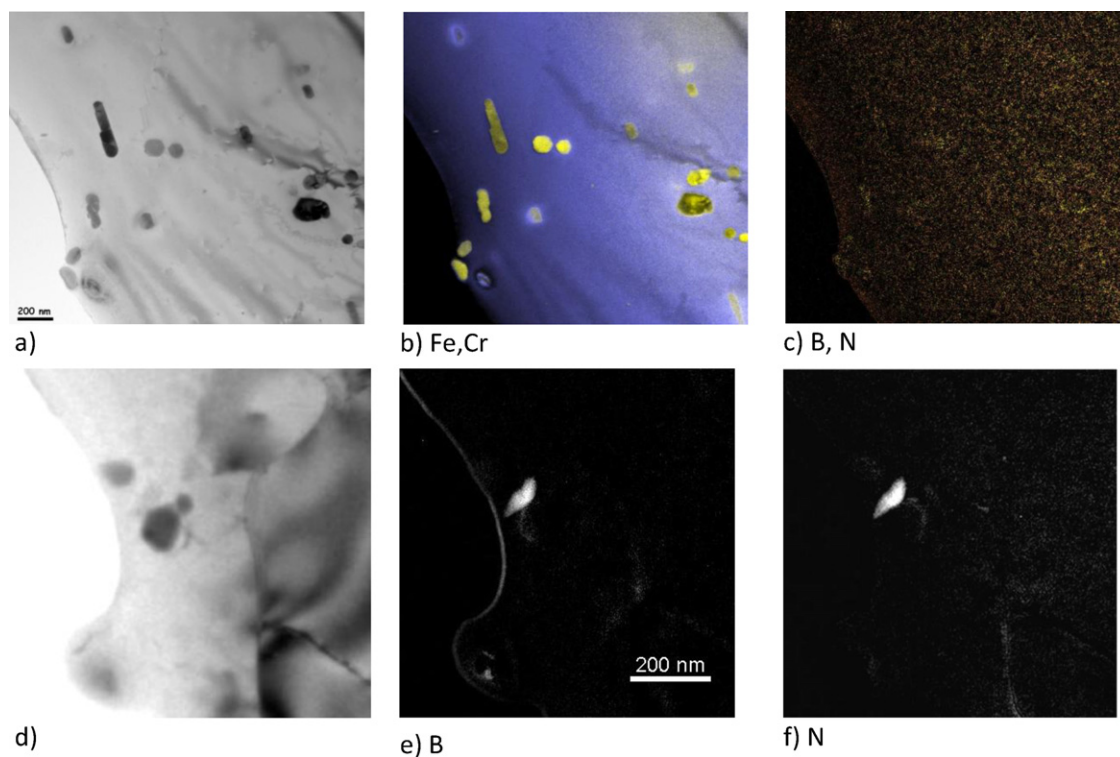


Fig. 8. (a) BF TEM image of ADS3 region with several precipitates. (b) Coloured overlay of iron and chromium EFTEM elemental maps taken from the same region as (a). Fe is displayed in blue and Cr in yellow. (c) Overlay of boron and nitrogen elemental maps. Since the B and N concentrations are below the detectable limit, the picture shows only noise. (d) BF TEM image of another region of ADS3. (e and f) Elemental maps of boron and nitrogen respectively. The EFTEM analysis reveals the presence of a BN-precipitate inside a region shown in (d).

7. Helium effects

Due to absence of irradiation facility with fusion reactor relevant neutron spectrum the helium effects are studied in different simulation experiments. Here the main outcomes of boron doping technique and spallation target irradiation are briefly summarized.

7.1. Boron doping technique

In irradiation experiments SPICE [7,8] and ARBOR [9,11] helium effects were studied by neutron irradiation of EUROFER97 based model steels doped with different contents of natural boron and separated ^{10}B -isotope. In SPICE programme the boron doped steels were irradiated at nominal irradiation temperatures (T_{irr}) of 250, 350 and 450 °C to a volume average damage dose of 16.3 dpa. In the ARBOR 1 and ARBOR 2 experiments the boron doped steels were irradiated in a temperature range of 332–338 °C to a damage dose of 22.4 and 69.8 dpa, respectively. Due to differences in the content of ^{10}B isotope and due to differences in the neutron spectra between HFR, Petten and BOR 60 reactors it was possible to generate helium in a wide concentration range between 10 and 432 appm.

Due to relatively low boron burn-up rate for BOR 60 irradiation the helium production rate can be considered to be nearly constant during the whole irradiation time of ARBOR 1 and ARBOR 2, see e.g. [26]. In contrast, according to the neutronics calculations of HFR-Petten, after ca. 1.6 dpa nearly all boron is burnt-up, see e.g. [27]. This implies that an initial irradiation phase which is characterized by a very high helium production rate superimposed on the dpa production is followed by a considerably longer irradiation phase characterized by dpa production only. Very high initial production rate of helium is expected to accelerate nucleation process of helium bubbles and to reduce fraction of helium atoms captured by microstructural sinks, e.g. by grain boundaries [28]. This will

lead to a lower peak bubble diameter and to a larger peak bubble concentration in comparison with a constant and lower helium production rate. The role of the resolution of helium from bubbles as a consequence of interaction of displacement cascades with bubbles as predicted by atomistic study, e.g. in [29] and as observed experimentally, e.g. in helium implanted and subsequently with 300 keV Fe^+ irradiated ferritic model alloy in [30] is not fully understood and has to be studied in more detail in the future.

High content of alloying element boron can severely affect the microstructure and mechanical properties of the steels already in the unirradiated condition either by formation of boron rich precipitates or by accumulation of boron at grain boundaries [31,32]. The investigation of the effect of the dopant boron on the microstructure of the selected 9%Cr martensitic steels was performed in [15,16] for boron contents between 5 and 1120 wppm. The study revealed strong degradation of the microstructure in the heat with 1120 wppm boron, characterized by a presence of high density of coarse (up to few μm large) Fe, Cr and B rich precipitates. In the case of 83 wppm ^{10}B doped alloy the presence of small (up to few hundred nm) BN and $(\text{Fe}, \text{Cr})_2\text{B}$ precipitates were reported in [15,16]. Boron distribution in 83 wppm ^{10}B doped model alloy (ADS3) was also studied in [33]. Fig. 8a shows a bright field (BF) Transmission Electron Microscopy (TEM) image of ADS3. Several precipitates of about one hundred nm sizes are visible. The Energy Filtered Transmission Electron Microscopy (EFTEM) elemental map in Fig. 8b reveals that they consist predominantly of Cr and Fe (and also carbon, not shown). Because the boron content is 10 times lower than the detectable limit of about 0.5 at.%, no signal can be seen in the EFTEM map in Fig. 8c. Only few precipitates were identified to be of BN type, e.g. in a region shown in Fig. 8d as was confirmed by the EFTEM analysis of elemental maps of boron (Fig. 8e) and nitrogen (Fig. 8f). For the region shown in Fig. 8d nearly all boron was estimated to be located within the

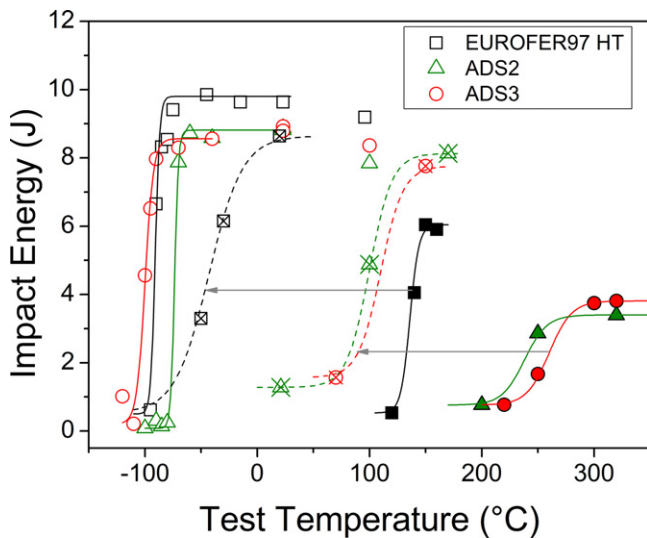


Fig. 9. Impact energy vs. test temperature for EUROFER97 HT, ADS2 and ADS3 in unirradiated (open symbols) condition, after neutron irradiation to 69.8 dpa at 332–338 °C (solid symbols) and after post irradiation annealing at 550 °C for 3 h (crossed symbols). The lines are fits to the ductile to brittle transition region. The arrows indicate recovery of the impact properties after post irradiation annealing.

BN precipitate [33]. As BN precipitates were observed only in a few cases it can be concluded that most of the boron is homogeneously distributed in the steel matrix or exists in too small precipitates/clusters to be detectable in EFTEM elemental maps. It is expected that the presence of large BN precipitates will have influence on the evolution of the helium microstructure locally.

Fig. 9 shows impact energy vs. test temperature curves for base EUROFER steel and two boron doped steels in the unirradiated condition, after neutron irradiation to 69.8 dpa at 332–338 °C and after post irradiation annealing at 550 °C for 3 h [11,22,24,34]. The comparison of the impact properties of boron doped steels and base EUROFER97 HT in the unirradiated state, indicated only minor influence of dopant boron on the impact properties with respect to both the DBTT and toughness [22,34]. The irradiated ADS2 (24 appm He) and ADS3 (120 appm He) steels show considerably larger embrittlement in comparison to base EUROFER97 HT which was attributed to helium effects [22,34]. As can be seen from Fig. 9 and as already reported in [24], the post irradiation annealing of EUROFER97 leads to a substantial recovery of the impact properties both with respect to DBTT and upper shelf energy indicating annealing of the displacement damage to a large extent. Furthermore, nearly complete recovery of the tensile properties of EUROFER97 was observed through post irradiation annealing in [24]. For the case of boron doped steels, however, the residual embrittlement after post irradiation annealing is considerably larger than the residual embrittlement for EUROFER97 HT indicating that helium effects cannot be annealed by applying post irradiation heat treatment [11].

Fig. 10 shows helium induced embrittlement, quantified as a DBTT shift in boron doped steel after subtraction of the corresponding dpa induced DBTT shift for reference EUROFER97 [22,3]. A progressive embrittlement with produced helium amount is seen for SPICE, ARBOR 1 and ARBOR 2 experiments in the irradiation temperature range between 250 and 350 °C. The embrittlement rate seems to be reduced at the achieved helium concentration. At $T_{irr} \leq 350$ °C and up to 420 appm He the helium embrittlement rate between 0.5 and 0.6 °C/appm He can be estimated from this boron doping experiment. This embrittlement rate is slightly higher than the embrittlement rate of 0.40 °C/appm He obtained at $T_{irr} = 250$ °C up to 300 appm He by comparative studies of neutron irradiation

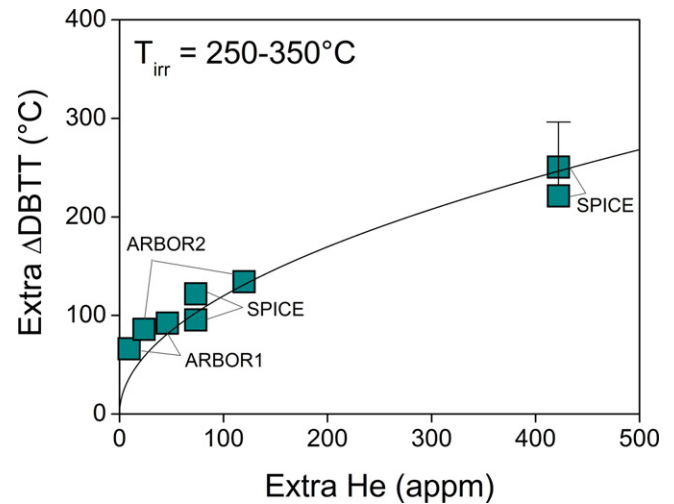


Fig. 10. Helium induced extra embrittlement vs. extra helium amount for irradiated boron doped steels. The line is a $A(p_{He})^{1/2}$ type least square fit to the data, with A as fitting parameter and p_{He} as helium concentration [3].

induced embrittlements in ^{11}B (F82H + 57 wppm ^{11}B + 200 wppm N) and ^{10}B (F82H + 59 wppm ^{10}B + 190 wppm N) isotopes doped F82H steels in [35].

The influence of the irradiation temperature on the embrittlement of boron doped steels is shown in Fig. 11 [34]. The helium induced extra embrittlement is comparable at irradiation temperatures of 250 and 350 °C. At $T_{irr} = 450$ °C, in contrast, helium effects are considerably reduced for the same helium contents. Indeed the DBTT of ADS2 (83 appm He) is comparable to the DBTT of base EUROFER steel (10 appm He) and the DBTT of ADS3 (432 appm He) is now considerably reduced in comparison to 250 and 350 °C irradiations. The comparison of embrittlement for base EUROFER and ADS3 steels at $T_{irr} = 450$ °C yields an extra helium induced embrittlement of 108.5 °C for 422 appm He (total helium amount of 432 appm produced in ADS3 is here corrected for helium amount of 10 appm generated in base EUROFER steel). Comparatively, at $T_{irr} = 250$ –350 °C the extra helium induced embrittlement for the same helium amount was estimated to be 220–250 °C. Such behaviour can be qualitatively understood by taking into account an evolution of helium microstructure in boron doped model steels. The distribution of helium bubbles was shown to

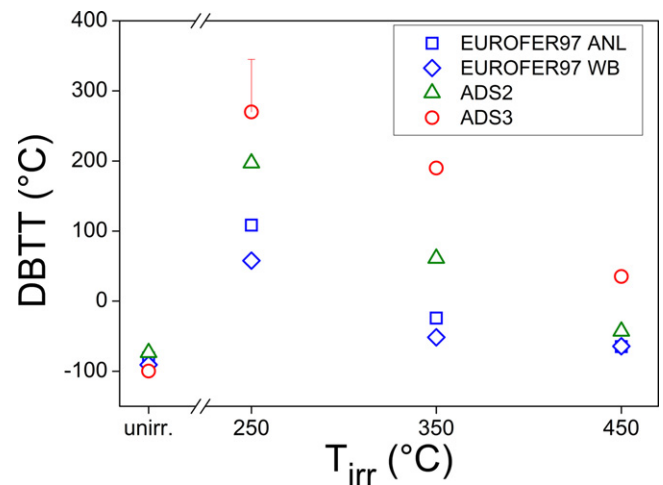


Fig. 11. DBTT vs. irradiation temperature for boron-doped and base EUROFER97 steels after irradiation in SPICE programme to volume average damage dose of 16.3 dpa [34]. For comparison the results in the unirradiated conditions are also indicated. The error bar indicates uncertainty in the DBTT of ADS3 at $T_{irr} = 250$ °C.

strongly depend on the irradiation temperature [3,36]. Namely, at $T_{\text{irr}} = 250^\circ\text{C}$ (SPICE) the microstructure of boron doped alloys was characterized by helium bubbles nearly homogeneously distributed in the steel matrix, whereas at $T_{\text{irr}} = 450^\circ\text{C}$ (SPICE) helium bubbles were non-homogeneously nucleated preferably at line dislocations [3,36]. A number of bubbles was less and bubble sizes were considerably larger at $T_{\text{irr}} = 450^\circ\text{C}$ in comparison to $T_{\text{irr}} = 250^\circ\text{C}$. Capturing of helium by line dislocations and evolution of fewer but larger bubbles at these sinks, thus considerably reduces helium induced embrittlement in boron doped model alloys. The helium embrittlement rate of about $0.25^\circ\text{C}/\text{appm He}$ is estimated up to 420 appm He for $T_{\text{irr}} = 450^\circ\text{C}$ from this boron doping experiment. This estimation can be considered as too conservative as the boron doping technique most probably overestimates helium embrittlement as a result of non-homogeneous distribution of boron, e.g. due to precipitation of boron nitrides [16,33] and due to possible segregation of boron at grain boundaries [31]. Furthermore, boron transmutation into helium also produces lithium as by-product. Chemical effect of lithium on the DBTT shift was assessed to be very small by comparison of DBTT shifts quantified in neutron irradiated boron doped F82H and helium implanted F82H steels [37]. The effect of lithium on cavity formation needs to be investigated in future for more accurate assessment of helium effects. The boron doping technique is not suited for the study of helium effects above 500 appm helium due to strong degradation of the microstructure by dopant boron [16].

7.2. Spallation target environment

Spallation neutron and proton irradiation is another technique frequently used for the study of helium effects. This simulation technique have some specific limitations, e.g. relatively large helium to dpa ratio of about 70 appm/dpa, simultaneous irradiation of sample with spallation neutrons and protons, variation of irradiation temperature due to variation of intensity of a proton beam, etc. Irradiation in the spallation target environment is consequently expected to overestimate helium effects. The assessment given below, thus has to be considered being too conservative.

Helium effects in structural materials have been intensively studied in e.g. [38,39] by irradiation in spallation targets. By comparison of DBTT shifts observed under spallation target and fission neutron irradiations at $T_{\text{irr}} < 380^\circ\text{C}$ it was found out, that the DBTT shift of the steels irradiated in spallation targets was much larger than that of neutron irradiated steels and the difference increased with irradiation dose which was attributed to the He-induced embrittlement effects [38,39]. At irradiation temperatures below 380°C the shifts in the DBTT due to synergy of helium and dpa effects was shown to linearly increase with helium concentration up to 1600 appm. For the case of EUROFER97 the embrittlement due to 18 dpa and 1400 appm helium under spallation target irradiation was about 600°C . Taking into account the displacement damage (18 dpa) induced low temperature ($T_{\text{irr}} \leq 335^\circ\text{C}$) embrittlement of about 190°C under fission neutron environment, see Fig. 6, helium induced embrittlement under spallation target environment can be estimated to be about 410°C for 1400 appm, which corresponds to the helium embrittlement rate of about $0.3^\circ\text{C}/\text{appm He}$ at $T_{\text{irr}} < 380^\circ\text{C}$. By considering a DEMO reactor relevant He/dpa ratio of 10 appm/dpa, the helium induced extra embrittlement of about $3^\circ\text{C}/\text{dpa}$ can be estimated up to 140 dpa. The helium induced embrittlement rate is, however, not constant and is reduced for lower helium contents. So up to 600 appm He the estimated embrittlement rate due to helium is reduced down to $0.13\text{--}0.15^\circ\text{C}/\text{appm He}$ at $T_{\text{irr}} < 380^\circ\text{C}$. For DEMO reactor relevant He/dpa ratio of 10 appm/dpa this will correspond to helium induced extra embrittlement of about $1.3\text{--}1.5^\circ\text{C}/\text{dpa}$ up to 60 dpa.

8. Swelling

In addition to helium embrittlement, fusion relevant helium production accelerated swelling has to be taken into account while discussing application potential of the RAFM steels. Several experiments simulating swelling in RAFM steels have been performed in the past including fission reactor irradiation of boron and nickel doped steels [40], irradiation under spallation target environment [38,41], multi-ion beam irradiation [42]. The swelling was shown to be very sensitive to irradiation or implantation temperature, helium and dpa production rates and steel virgin microstructure. So, neutron irradiation of boron and nickel doped F82H based steels to 51 dpa at 300°C yielded nearly no swelling up to 504 appm He [40]. After irradiation at 400°C , however, 1.2% and 1.1% volumetric swelling was observed in F82H+60 wppm nat. B and F82H+58 wppm ^{10}B doped steels due to production of 77 and 332 appm He, respectively [40]. Remarkably, about 0.5% swelling was determined in reference F82H std. steel due to 25 appm He only [40]. Such a large swelling was attributed to a non-controlled helium production-to-dpa rate under neutron irradiation of boron doped steels [42]. In contrast to boron doped steels the nickel doped F82H + 1.31 at.% 58Ni steel exhibited no swelling even though about 504 appm He was generated due to transmutation of ^{58}Ni isotope. Different effects of boron and nickel doping on the microstructure have to be taken into account for the assessment of helium effects. Whereas microstructures of boron doped specimens were reported to be very similar to that of base F82H steel, the microstructures of the un-tempered Ni-doped specimens were reported to be different from that of base steel [40]. An increase of a number density of MC carbides in comparison to reference F82H steel was identified. Furthermore, formation of a high density of precipitates, mainly of M_6C type was observed under neutron irradiation in 60Ni and 58Ni doped steels [40]. This process was attributed to the presence of high concentration of carbon atoms in the un-tempered steel matrix. Reduction of the vacancy mobility due to strong interaction with carbon atoms was considered as a main reason for swelling suppression in neutron irradiated nickel doped steels in [40]. Single, dual and triple beam irradiation of F82H specimens were performed for the study of the effects of gas atoms and displacement damage on the mechanical properties and microstructure of F82H [42]. The peak temperature of swelling induced by dual beam irradiation (10.5 MeV Fe^{3+} and 1.05 MeV He^+) to 50 dpa at helium to dpa ratio of 10 appm He/dpa was at about 430°C in the temperature range from 360 to 600°C and the value of swelling was 0.6% [42]. A well pronounced bimodal distribution observed at 430°C indicated, advanced bubble to void transformation. The observed swelling of 0.6% is still in the acceptable range according to the French design code RCC-MRX. It has to be emphasized, however, that whereas He/dpa ratio of 10 studied in [42] is adequate for fusion condition, the implied dpa production rate of $1.0 \times 10^{-3}\text{ dpa/s}$ is at least three orders of magnitude larger than the damage accumulation rate under fusion neutron spectrum. The absence of irradiation facility with fusion relevant neutron spectrum does not allow the assessment of swelling under in-service condition as there still remain uncertainty in the helium content and irradiation temperature for the onset of pronounced swelling for fusion relevant dpa and helium accumulation rates.

9. Design limitations due to dpa and helium

The European reference RAFM steel EUROFER97 shows excellent mechanical properties in the unirradiated condition from -80 up to 550°C [1,4]. Above this temperature range the structural application of the steel is limited mainly by considerable loss of tensile and creep strengths [1,4]. Furthermore, strong hardening

and correlated embrittlement induced by low temperature neutron irradiation ($T_{\text{irr}} \leq 335^\circ\text{C}$) imposes a low application temperature limit for EUROFER97 [7,8,43]. Only minor hardening and embrittlement observed at $T_{\text{irr}} = 350^\circ\text{C}$ indicates considerable healing of radiation damage at this temperature [7,8,43]. Neutron irradiation at $T_{\text{irr}} \geq 400^\circ\text{C}$ has nearly no impact on the mechanical properties [7,8,43]. On the basis of these experiments EUROFER97 is highly suited for special fusion reactor design with the operating temperature range between 350 and 550°C for the FW and BB structures.

In the irradiation temperature range between 350 and 550°C the application of EUROFER97 will be further limited by helium effects. By assessment of helium embrittlement of between 0.15 and $0.25^\circ\text{C}/\text{appm He}$ on the base of helium simulation experiments [2,22,34,38,39] and for fusion reactor relevant helium to dpa ratio of 10 appm He/dpa, helium effects are expected to be tolerable up to a damage dose of at least 40 dpa. Consequently, application temperature range and DPA and He limits for EUROFER97 are proposed between 350 and 550°C and 40 dpa and 400 appm He, respectively.

At low irradiation temperatures ($T_{\text{irr}} < 350^\circ\text{C}$) the mechanical performance of RAFM steel will be mainly limited by dpa effects. The dpa induced low temperature embrittlement can be largely recovered through application of post irradiation annealing. In contrast to dpa damage the helium effects cannot be recovered through post irradiation annealing, see Fig. 9 and [11]. By utilizing post irradiation annealing for the recovery of dpa effects at low irradiation temperatures in FW and BB structures and for fusion reactor relevant helium to dpa ratio of 10 appm He/dpa the helium effects will be tolerable up to a damage dose of at least 40 dpa on the basis of spallation proton irradiation experiments.

10. Conclusions

The main objective of the current work was the analysis of the key issues related to neutron irradiation on blanket and divertor materials. The assessment of the mechanical properties of European reduced activation ferritic/martensitic steel EUROFER97 and its ODS variants has been performed up to a damage dose of 80 dpa. The main conclusions of the assessment can be summarized as follows

- Low temperature neutron irradiation ($T_{\text{irr}} \leq 335^\circ\text{C}$) leads to strong hardening and embrittlement of EUROFER97 and other international RAFM steels. Minor hardening and embrittlement observed at $T_{\text{irr}} = 350^\circ\text{C}$ indicates considerable healing of radiation damage. Neutron irradiation at $T_{\text{irr}} \geq 400^\circ\text{C}$ has nearly no impact on the mechanical properties. Detailed microstructural analysis of neutron irradiated specimens is required for deeper understanding of the nature of the radiation damage in RAFM steels.
- The increase of the Yield Stress of RAFM steels is rather steep at doses below 10 dpa at $T_{\text{irr}} \leq 335^\circ\text{C}$. In spite of large scattering of low temperature, high dose hardening data a clear reduction of the hardening per dose increment is observed at achieved damage doses of 70–80 dpa. Selected RAFM steels (e.g. EUROFER97, Heat E83697) show saturation of hardening at 70 dpa. Ductility properties (Uniform Strain, Total Strain) seem to saturate already above 2.5 dpa. Lack of irradiated specimens does not allow detailed statistical analysis of the results.
- All investigated RAFM steels show steep increase in the ΔDBTT with dose below 15 dpa at $T_{\text{irr}} \leq 335^\circ\text{C}$. At 70 dpa EUROFER97 and other RAFM steels indicate saturation behaviour of low temperature embrittlement.
- Progressive material embrittlement, quantified as increase in FTTT, observed for EUROFER97 indicate no saturation of FTTT for the achieved damage doses of 10 dpa. Comparison of low temperature neutron irradiation ($T_{\text{irr}} \leq 335^\circ\text{C}$) induced shifts in

FTTT and in Charpy DBTT reveals non-conservative estimation of the embrittlement by Charpy impact test. There is a need for high dose fracture toughness experiments on EUROFER97.

- Post irradiation annealing at 550°C for 3 h leads to a nearly complete recovery of the impact and tensile properties of low temperature ($T_{\text{irr}} = 335^\circ\text{C}$) irradiated EUROFER97 indicating substantial healing of radiation defects. Helium effects cannot be healed out by post irradiation annealing.
- Helium effects are not sufficiently understood due to absence of an irradiation facility with fusion reactor relevant neutron spectrum and have to be a subject of future investigations. Different simulating techniques used, e.g. fission reactor irradiation of boron doped model steels or spallation neutron and proton irradiation of RAFM steels most probably strongly overestimate helium effects. Moreover, helium effects will strongly depend on the irradiation temperature. Boron doping technique yielded progressive embrittlement with increasing helium concentration (10–430 appm) at $T_{\text{irr}} \leq 350^\circ\text{C}$, the embrittlement rate was however reduced at achieved helium contents. Helium embrittlement was considerably reduced at $T_{\text{irr}} = 450^\circ\text{C}$. Synergistic helium and dpa effects under spallation target environment at $T_{\text{irr}} \leq 380^\circ\text{C}$ yielded linear increase of DBTT shift with produced helium up to 1600 appm.
- The RAFM steels are highly suited for the special fusion reactor design with the operating temperature range between 350 and 550°C for the FW and BB. By considering DEMO relevant helium to dpa ratio of 10 appm/dpa helium effects will be tolerable up to a damage dose of 40 dpa and up to helium contents of 400 appm He in the temperature window between 350 and 550°C . The mechanical performance of RAFM steel at low irradiation temperatures ($T_{\text{irr}} < 350^\circ\text{C}$) will be mainly limited by dpa induced embrittlement. By utilizing post irradiation annealing of FW and BB structures for the recovery of dpa effects at low irradiation temperatures the helium effects will be tolerable up to a damage dose of at least 40 dpa.
- Irradiation behaviour with respect to impact properties is rather poor for early developed ODS EUROFER steels. Though low temperature irradiation behaviour ($T_{\text{irr}} < 340^\circ\text{C}$) is considerably improved at low doses for recently developed ODS EUROFER steels there is still a need for further improvement of irradiation resistance. Recent development ODS EUROFER steel with 0.3 wt.% Y_2O_3 shows no degradation of mechanical properties after neutron irradiation up to 3 dpa at 450 and 550°C . There is a need for (high dose) irradiation data on novel ODS EUROFER steels.
- The conclusions given above are made on the basis of irradiation behaviour of base RAFM steels. Qualification of advanced joining technologies (e.g. diffusion bonding, EB/TIG welding) under high dose irradiation damage is an important requirement for disturbance free operation of DEMO and belongs to the key priorities within structural materials R&D.

Acknowledgements

This work, supported by the European Communities under the contract of Association between EURATOM and Karlsruhe Institute of Technology, was carried out within the framework of the European Fusion Development Agreement. The views and opinions expressed herein do not necessarily reflect those of the European Commission.

References

- [1] A. Möslang, E. Diegele, M. Klimiankou, R. Lässer, R. Lindau, E. Lucon, E. Materna-Morris, C. Petersen, R. Pippan, J.W. Rensman, M. Rieth, B. van der Schaaf, H.-C. Schneider, F. Tavassoli, Towards reduced activation structural materials data for fusion DEMO reactors, *Nuclear Fusion* 45 (2005) 649–655.

- [2] P. Norajitra, R. Giniyatulin, N. Holstein, T. Ihli, W. Krauss, R. Kruessmann, V. Kuznetsov, I. Mazul, I. Ovchinnikov, B. Zeep, Status of He-cooled divertor development for DEMO, *Fusion Engineering and Design* 75–79 (2005) 307–311.
- [3] E. Gaganidze, C. Petersen, E. Materna-Morris, C. Dethloff, O.J. Weiß, J. Aktaa, A. Povstyanko, A. Fedoseev, O. Makarov, V. Prokhorov, Mechanical properties and TEM examination of RAFM steels irradiated up to 70 dpa in BOR 60, *Journal of Nuclear Materials* 417 (2011) 9.
- [4] R. Lindau, A. Möslang, M. Rieth, M. Klimiankou, E. Materna-Morris, A. Alamo, et al., Present development status of EUROFER and ODS for application in blanket concepts, *Fusion Engineering and Design* 75–79 (2005) 989–996.
- [5] E. Lucon, R. Chaouadi, M. Decréton, Mechanical properties of the European reference RAFM steel (EUROFER97) before and after irradiation at 300 °C, *Journal of Nuclear Materials* 329–333 (2004) 1078–1082.
- [6] J. Rensman, NRG Irradiation Testing: Report on 300 °C and 60 °C Irradiated RAFM Steels, NRG Petten, 2002/05.68497/P, (2005).
- [7] E. Gaganidze, B. Dafferner, H. Ries, R. Rolli, H.-C. Schneider, J. Aktaa Irradiation Programme HFR Phase IIb (SPICE), Impact Testing on up to 16.3 dpa Irradiated RAFM Steels, Forschungszentrum Karlsruhe, FZKA 7371, April 2008.
- [8] E. Materna-Morris, A. Möslang, H.-C. Schneider, Tensile and Low Cycle Fatigue Properties of EUROFER97-Steel after 16.3 dpa Neutron-Irradiation at 523, 623 and 723 K, accepted for publication in *Journal of Nuclear Materials* (2013).
- [9] C. Petersen, Post Irradiation Examination of RAF/M Steels after Fast Reactor Irradiation up to 33 dpa and <340 °C (ARBOR 1), *Karlsruher Institut für Technologie, FZKA 7517*, 2010.
- [10] A. Alamo, J.L. Bertin, V.K. Shamardin, P. Wident, Mechanical properties of 9Cr martensitic steels and ODS-FeCr alloys after neutron irradiation at 325 °C up to 42 dpa, *Journal of Nuclear Materials* 367–370 (2007) 54–59.
- [11] E. Gaganidze, C. Petersen, Post Irradiation Examination of RAFM Steels after Fast Reactor Irradiation up to 71 dpa and <340 °C (ARBOR 2), *Karlsruhe Institute of Technology, KIT Scientific Report 7596*, 2011.
- [12] J. Henry, X. Averty, A. Alamo, Tensile and impact properties of 9Cr tempered martensitic steels and ODS-FeCr alloys irradiated in a fast reactor at 325 °C up to 78 dpa, *Journal of Nuclear Materials* 417 (2011) 99–103.
- [13] R. Lindau, A. Möslang, M. Schirra, P. Schlossmacher, M. Klimenkov, Mechanical and microstructural properties of a hipped RAFM ODS-steel, *Journal of Nuclear Materials* 307–311 (2002) 769–772.
- [14] N.V. Luzginova, H.S. Nolles, P. ten Pierick, T. Bakker, R.K. Mutnuru, M. Jong, D.T. Blagoeva, Irradiation response of ODS Eurofer97 steel, *Journal of Nuclear Materials* 428 (2012) 192–196.
- [15] P. Graf, H. Zimmermann, E. Nold, E. Materna-Morris, A. Möslang, Der Einfluss von Bor auf die Gefügeeigenschaften von martensitischen 9%-Chromstählen, Sonderbände der Metallographie, in: P. Portella (Ed.), *Fortschritte in der Metallographie: Vortragstexte der 37. Metallographie-Tagung*, vol. 35, Berlin, 17–19 September 2003, 2004, pp. S71–S76.
- [16] E. Materna-Morris, M. Klimenkov, A. Möslang, The influence of boron on structural properties of martensitic 8–10%-steels, *Materials Science Forum* 730–732 (2013) 877–882.
- [17] C. Petersen, J. Aktaa, E. Diegele, E. Gaganidze, R. Lässer, E. Lucon, E. Materna-Morris, A. Möslang, A. Povstyanko, V. Prokhorov, J. Rensman, B. van der Schaaf, H.-C. Schneider, Mechanical properties of reduced activation ferritic/martensitic steels, in: *Proceedings of 21st IAEA Fusion Energy Conference*, Chengdu, China, October 16–21, 2006, FT/1-4Ra.
- [18] E. Gaganidze, H.-C. Schneider, C. Petersen, J. Aktaa, A. Povstyanko, V. Prokhorov, R. Lindau, E. Materna-Morris, A. Möslang, E. Diegele, R. Lässer, B. van der Schaaf, E. Lucon, Mechanical properties of reduced activation ferritic/martensitic steels after high dose neutron irradiation, in: *Proceedings of 22nd IAEA Fusion Energy Conference*, Geneva, Switzerland, October 13–18, 2008, FT/P 2-1.
- [19] E. Lucon, W. Vandermeulen, Overview of the tensile properties of EUROFER in the unirradiated and irradiated conditions, *Journal of Nuclear Materials* 386–388 (2009) 254–256.
- [20] E. Lucon, W. Vandermeulen, Overview and Critical Assessment of the Tensile Properties of Unirradiated and Irradiated EUROFER97, Open report SCK-CEN-BLG-1042 REV(1), 2007.
- [21] A.D. Whapham, M.J. Makin, The hardening of lithium fluoride by electron irradiation, *Philosophical Magazine* 5 (51) (1960) 237–250.
- [22] E. Gaganidze, C. Petersen, J. Aktaa, Study of helium embrittlement in boron doped EUROFER97 steels, *Journal of Nuclear Materials* 386–388 (2009) 349–352.
- [23] G.R. Odette, D. Frey, Development of mechanical property correlation methodology for fusion environment, *Journal of Nuclear Materials* 85–86 (1979) 817–822.
- [24] E. Gaganidze, C. Petersen, E. Materna-Morris, C. Dethloff, O.J. Weiß, J. Aktaa, A. Povstyanko, et al., Mechanical properties and TEM examination of RAFM steels irradiated up to 70 dpa in BOR 60, *Journal of Nuclear Materials* 417 (2011) 93–98.
- [25] E. Gaganidze, Assessment of Fracture Mechanical Experiments on Irradiated EUROFER97 and F82H Specimens, *Forschungszentrum Karlsruhe, Wissenschaftliche Berichte, FZKA 7310*, 2007.
- [26] E. Gaganidze, C. Dethloff, O.J. Weiß, V. Svetukhin, M. Tikhonchev, J. Aktaa, Modeling and TEM investigation of helium bubble growth in RAFM steels under neutron irradiation, *Journal of ASTM International* (2012), <http://dx.doi.org/10.1520/STP103972>.
- [27] M. Rieth, B. Dafferner, H.-D. Röhrig, Embrittlement behaviour of different inter-nuclear low activation alloys after neutron irradiation, *Journal of Nuclear Materials* 258–263 (1998) 1147–1152.
- [28] C. Dethloff, E. Gaganidze, V.V. Svetukhin, J. Aktaa, Modeling of helium bubble nucleation and growth in neutron irradiated boron doped RAFM steels, *Journal of Nuclear Materials* 426 (2012) 287–297.
- [29] R.E. Stoller, D.M. Stewart, An atomistic study of helium resolution in bcc iron, *Journal of Nuclear Materials* 417 (2011) 1106–1109.
- [30] H. Trinkaus, The effect of cascade induced gas resolution on bubble formation in metals, *Journal of Nuclear Materials* 318 (2003) 234–240.
- [31] R.L. Klueh, D.S. Gelles, S. Jitsukawa, A. Kimura, G.R. Odette, B. van der Schaaf, M. Victoria, Ferritic/martensitic steels—overview of recent results, *Journal of Nuclear Materials* 307–311 (2002) 455–465.
- [32] T. Yamamoto, G. Odette, H. Kishimoto, J.-W. Rensman, P. Miao, On the effects of irradiation and helium on the yield stress changes and hardening and non-hardening embrittlement of ~8Cr tempered martensitic steels: compilation and analysis of existing data, *Journal of Nuclear Materials* 356 (2006) 27–49.
- [33] O. Weiß, E. Gaganidze, C. Dethloff, Quantitative TEM & SEM investigation of irradiated specimens from SPICE (HFR) and ARBOR 1 (Bor-60), *Nuclear Fusion Programme, Annual Report of the Association Karlsruhe Institute of Technology/EURATOM, KIT SCIENTIFIC Reports 7548*, January 2009–December 2009, pp. 204–207.
- [34] E. Gaganidze, J. Aktaa, The effects of helium on the embrittlement and hardening of boron doped EUROFER97 steels, *Fusion Engineering and Design* 83 (2008) 1498–1502.
- [35] E. Wakai, N. Okubo, M. Ando, T. Yamamoto, F. Takada, Reduction method of DBTT shift due to irradiation for reduced-activation ferritic/martensitic steels, *Journal of Nuclear Materials* 398 (2010) 64–67.
- [36] E. Materna-Morris, A. Möslang, H.-C. Schneider, R. Rolli, Microstructure and tensile properties in reduced activation 8–9%Cr steels at fusion relevant He/dpa ratios, dpa rates and irradiation temperatures, in: *Proceedings of 22nd IAEA Fusion Energy Conference*, Geneva, Switzerland, October 13–18, 2008, FT/P2-2.
- [37] E. Wakai, S. Jitsukawa, H. Tomita, K. Furuya, M. Sato, K. Oka, et al., Radiation hardening and embrittlement due to He production in F82H steel irradiated at 250 °C in JMTR, *Journal of Nuclear Materials* 343 (2005) 285–296.
- [38] Y. Dai, W. Wagner, Materials researches at the Paul Scherrer Institute for developing high power spallation targets, *Journal of Nuclear Materials* 389 (2009) 288–296.
- [39] Y. Dai, J. Henry, Z. Tong, X. Averty, J. Malaplate, B. Long, Neutron/proton irradiation and He effects on the microstructure and mechanical properties of ferritic/martensitic steels T91 and EM10, *Journal of Nuclear Materials* 415 (2011) 306–310.
- [40] E. Wakai, N. Hashimoto, Y. Miwa, J.P. Robertson, R.L. Klueh, K. Shiba, S. Jitsukawa, Effect of helium production on swelling of F82H irradiated in HFIR, *Journal of Nuclear Materials* 283–287 (2000) 799–805.
- [41] X. Jia, Y. Dai, Microstructure of the F82H martensitic steel irradiated in STIP-II up to 20 dpa, *Journal of Nuclear Materials* 356 (2006) 105–111.
- [42] E. Wakai, M. Ando, T. Sawai, K. Kikuchi, K. Furuya, M. Sato, et al., Effect of gas atoms and displacement damage on mechanical properties and microstructures of F82H, *Journal of Nuclear Materials* 356 (2006) 95–104.
- [43] E. Gaganidze, H.-C. Schneider, B. Dafferner, J. Aktaa, High-dose neutron irradiation embrittlement of RAFM steels, *Journal of Nuclear Materials* 355 (2006) 83–88.